

REPORT DOCUMENTATION PAGE			Form Approved OMB NO. 0704-0188		
<p>The public reporting burden for this collection of information is estimated to average 1 hour per response, including the time for reviewing instructions, searching existing data sources, gathering and maintaining the data needed, and completing and reviewing the collection of information. Send comments regarding this burden estimate or any other aspect of this collection of information, including suggestions for reducing this burden, to Washington Headquarters Services, Directorate for Information Operations and Reports, 1215 Jefferson Davis Highway, Suite 1204, Arlington VA, 22202-4302. Respondents should be aware that notwithstanding any other provision of law, no person shall be subject to any penalty for failing to comply with a collection of information if it does not display a currently valid OMB control number.</p> <p>PLEASE DO NOT RETURN YOUR FORM TO THE ABOVE ADDRESS.</p>					
1. REPORT DATE (DD-MM-YYYY)		2. REPORT TYPE		3. DATES COVERED (From - To)	
		Technical Report		-	
4. TITLE AND SUBTITLE Silicon/Carbon Anodes with One-Dimensional Pore Structure for Lithium-Ion Batteries			5a. CONTRACT NUMBER		
			W911NF-11-1-0231		
			5b. GRANT NUMBER		
			5c. PROGRAM ELEMENT NUMBER		
			611102		
6. AUTHORS Yunhua Xu and Chunsheng Wang			5d. PROJECT NUMBER		
			5e. TASK NUMBER		
			5f. WORK UNIT NUMBER		
7. PERFORMING ORGANIZATION NAMES AND ADDRESSES			8. PERFORMING ORGANIZATION REPORT NUMBER		
University of Maryland - College Park Research Admin. & Advancement University of Maryland College Park, MD 20742 -5141					
9. SPONSORING/MONITORING AGENCY NAME(S) AND ADDRESS(ES) U.S. Army Research Office P.O. Box 12211 Research Triangle Park, NC 27709-2211			10. SPONSOR/MONITOR'S ACRONYM(S) ARO		
			11. SPONSOR/MONITOR'S REPORT NUMBER(S) 59134-CH.1		
12. DISTRIBUTION AVAILABILITY STATEMENT Approved for public release; distribution is unlimited.					
13. SUPPLEMENTARY NOTES The views, opinions and/or findings contained in this report are those of the author(s) and should not be construed as an official Department of the Army position, policy or decision, unless so designated by other documentation.					
14. ABSTRACT A series of composite electrode materials have been synthesized and characterized for lithium ion and sodium ion batteries. First, carbon-coated one-dimensional mesoporous (porous size: 50 nm) Si films was synthesized by electrochemical etching of crystalline silicon followed by CVD carbon coating. The one-dimension pore structure and carbon coating offer additional space and electric pathway to accommodate volume change and improve rate capability. The reversible capacity of over 1500 mAh/g was measured. Second, porous carbon/Si or Sn composites					
15. SUBJECT TERMS porous C/Si composite, porous C/Sn composite anodes, porous C/S cathodes, Li-ion battery, electrochemical performance					
16. SECURITY CLASSIFICATION OF:		17. LIMITATION OF ABSTRACT	15. NUMBER OF PAGES	19a. NAME OF RESPONSIBLE PERSON	
a. REPORT	b. ABSTRACT	c. THIS PAGE	UU	Chunsheng Wang	
UU	UU	UU		19b. TELEPHONE NUMBER	
			301-405-0352		

Report Title

Silicon/Carbon Anodes with One-Dimensional Pore Structure for Lithium-Ion Batteries

ABSTRACT

A series of composite electrode materials have been synthesized and characterized for lithium ion and sodium ion batteries. First, carbon-coated one-dimensional mesoporous (pore size: 50 nm) Si films was synthesized by electrochemical etching of crystalline silicon followed by CVD carbon coating. The one-dimension pore structure and carbon coating offer additional space and electric pathway to accommodate volume change and improve rate capability. The reversible capacity of over 1500 mAh/g was measured. Second, porous carbon/Si or Sn composites were synthesized by dispersing Sn or Si nanoparticles into soft-template polymer matrix followed by carbonization. These composites show enhance electrochemical performance compared to bare Si or Sn nanoparticles because the unique porous carbon structure provides space and mechanical support to accommodate the volume expansion and release stress/strain during electrochemical lithiation/delithiation. Third, homogenous Sn/C nanocomposite spheres were also synthesized using a spray pyrolysis method. Very small Sn nanoparticles (~ 10 nm) were uniformly dispersed in carbon spheres with diameter of about 400 nm. This composite spheres displayed superior cycling performance with no capacity fading after 10 cycles due to small size and uniform distribution of tin nanoparticles in carbon frame. Forth, nano-sulfur dispersed mesoporous carbon electrode materials were synthesized by high temperature S infusing method. The electrochemical properties were evaluated for lithium ion and sodium ion batteries. It is found that the nano-sulfur dispersed mesoporous carbon electrode materials show excellent electrochemical performance bouth for both Li ion and Na ion batteries, making is attractive cathodes for next generation of rechargeable batteries. This is the first time to investigate the electrochemical properties of sulfur cathode for both Li ion and Na ion batteries.

In Year Two, fundamental research on the porous C/Si, C/Sn, and C/S synthesized in Year One will be conducted and following science questions will be answered.

1. How do porosity and pore size of the C/Si and C/Sn composites affect the electrochemical performance?
2. How do the particle size of nanoparticle and the carbon ration in the C/Si and C/Sn composites affect the cycling stability?
3. What is the reaction mechanism of C/S cathodes in lithium ion and sodium ion batteries?

**Silicon/Carbon Anodes with One-Dimensional Pore Structure for Lithium-Ion
Batteries**

Grant # W911NF1110231

Annual Progress report

June 28, 2011 to February 28, 2012

Submitted to

Dr. Robert Mantz
Program Manager, Electrochemistry and Catalysis
Army Research Office
robert.a.mantz.civ@mail.mil
919-549-4309

Submitted by:

Chunsheng Wang, Ph.D.
Principal Investigator
Department of Chemical and Biomolecular Engineering
University of Maryland
College Park, Maryland 20740
Phone: 301-405-0352
cswang@umd.edu

Progress Reports

1. Objective

The objectives of this project in the first year are to develop porous Si/C and Sn/C composite anode materials for high performance lithium ion batteries and to investigate the mechanism how the porous carbon matrix enhances the cycling stability of Si and Sn anodes.

2. Summary of accomplishments in Year One

- Synthesis and characterization of carbon-coated one-dimensional mesoporous (porous size: 50 nm) Si films by electrochemical etching of crystalline silicon followed by CVD carbon coating.
- Synthesis and characterization of nano-Si dispersed mesoporous carbon electrode materials by carbonization of Si/copolymer.
- Synthesis and characterization of nano-Sn dispersed mesoporous carbon electrode materials by carbonization of Si/copolymer.
- Synthesis and characterization of nano-sulfur dispersed mesoporous carbon electrode materials by high temperature S infusing.
- Evaluation of the electrochemical performance of these four C/Si, C/Sn nanoporous composite materials for Li-ion batteries
- Evaluation of the electrochemical performance of C/S cathodes for Li-ion and Na-ion batteries.

3. Achievements

- *Yunhua Xu, Juchen Guo and Chunsheng Wang*, “Sponge-like porous carbon/tin composite anode materials for lithium ion batteries,” Submitted to Journal of Materials Chemistry, January, 2012
- *Yunhua Xu, and Chunsheng Wang*, C/Sn nanocomposite anode for Li-ion and Na-ion batteries. In preparation

4. Details accomplishments for Reporting Period

4.1 Carbon-coated one-dimensional mesoporous Si films

Synthesis and characterization

Porous silicon is fabricated by electrochemical etching of crystalline silicon, which produces a nanoporous skeleton comprised of silicon and air. The typical pore size formed in this process ranges from 5–100 nm, depending on the etching chemistry and substrate doping. Carbon was coated on the surface of pores using CVD.

The structure of the carbon-coated porous Si was examined by scanning electron microscopy (SEM) (Figure 1). Figure 1a shows that the carbon-coated porous Si has a well-aligned one dimensional pore structure. The pore diameter is less than 50 nm and the wall thickness is only a couple of nanometers. The thickness of the carbon layer is estimated to be about 10 nm. The carbon coating quality was checked by energy dispersive spectroscopic (EDS) mapping (Figure 2b). It is found that carbon is uniformly distributed through the whole pore structure, indicating that the CVD coating technique is an efficient method for one dimensional pore structure. The one dimensional carbon coated pore structure has several advantages over other porous structures. First, it provides large space to accommodate volume change during cycling processes. Second, the carbon layer not only acts as a conductive agent to improve the electronic property but also benefits to release the strain/stress induced from lithium insertion/extraction. Third, large surface area provides a large contact with electrolyte and enhances the kinetics as well as rate capability.

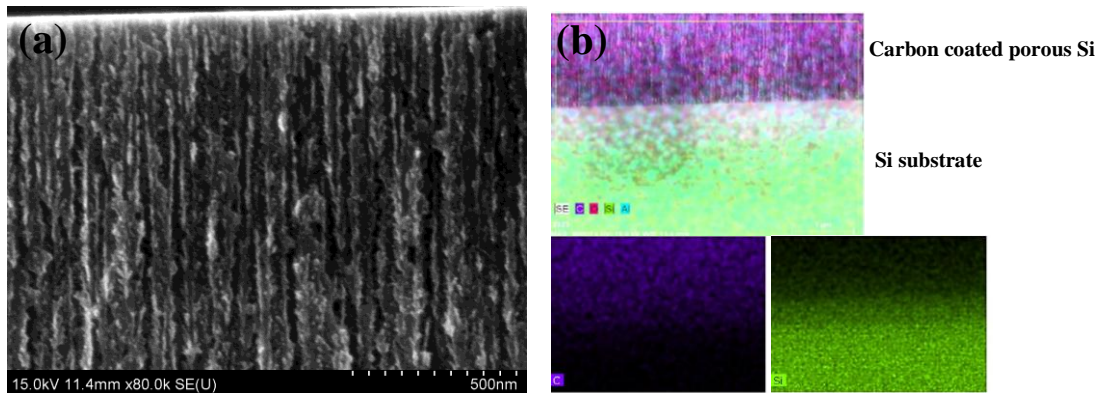


Figure 1. (a) SEM and (b) EDS elemental mapping images of the carbon-coated porous Si.

Electrochemical performance

It has been reported that the nanowell-array patterned Si anodes have better electrochemical performance over nanowire-arrays. The improved electrochemical properties of the patterned Si electrodes were attributed to the low internal resistance, fast charge transport, and facile stress relaxation. As a result, the nanostructure-patterned Si

electrodes exhibit superior Li storage capacity, high rate capability, and long cycling properties.

In this work, the carbon-coated one dimensional porous Si was tested in a coin-style half cell using Li as the counter electrode. Free-standing carbon-coated porous Si films were directly used as anode electrode without use of binder and conductive agent materials. 1M LiPF₆ in a mixture of ethylene carbonate/diethyl carbonate (EC/DEC, 1:1 by volume) and Celgard®3501 (Celgard, LLC Corp., USA) were used as electrolyte and separator, respectively. Electrochemical performance was tested using an Arbin battery test station (BT2000, Arbin Instruments, USA). Batteries were scanned between 0.02 – 1.5 V at the current density of 100 mA/g. Capacity was calculated on the basis of total mass of the carbon and porous Si.

Figure 2 shows the electrochemical properties of the carbon-coated porous Si. The reversible capacity is over 1500 mAh/g at the first cycle. The capacity increases in the first three cycles, and then begin to decrease, and stabilize at 1350 mAh/g after 10 cycles. Figure 2b shows the charge/discharge profiles at the first two cycles. An irreversible capacity of 1300 mAh/g was observed, which is due to the formation of a large amount of solid-electrolyte interface (SEI) film on the surface of the pores. The second discharge curve is almost the same as the curve in the first charge, indicating a good reversibility of the carbon-coated porous Si anode. The effect of pore size on the cycling stability is under investigation.

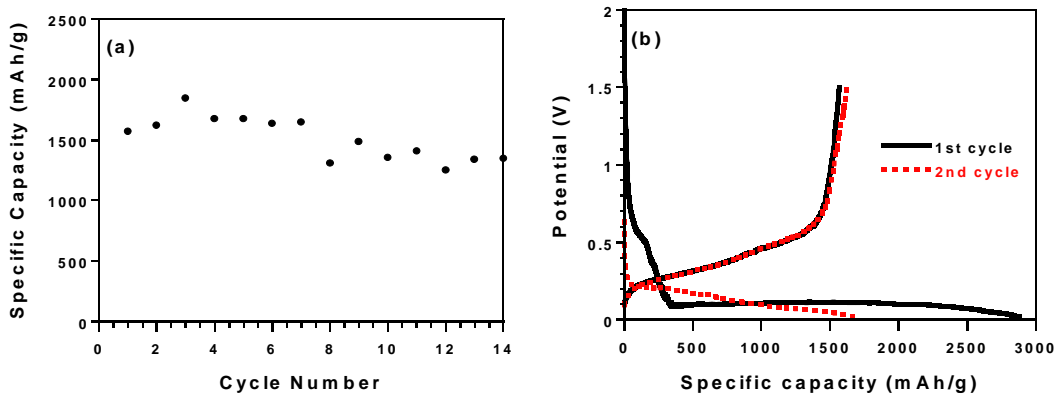


Figure 2. (a) Cycling performance and (b) charge/discharge profiles in the initial 2 cycles of the porous C/Si composite.

4.2. Nano-Si dispersed mesoporous carbon electrode materials

Synthesis and characterization

The synthesis of a nano-Si dispersed mesoporous carbon matrix consisted of three steps: preparation of polymer solution, Si nanoparticle dispersion, and carbonization. Si nanoparticles were obtained from Nanostructured & Amorphous Materials, Inc. (USA). All other materials were purchased from Sigma-Aldrich and were used without further purification. The polymer solution was prepared by dissolving resorcinol (R), triblock copolymer (Pluronic F127) and 37% HCl solution in *N,N*-dimethylformamide (DMF), where the triblock copolymer and HCl functioned as soft-template and catalyst, respectively. When the solution was clear, 37% formaldehyde (F) aqueous solution was added. After 30 minutes of vigorous stirring, the solution was stirred for another 30 minutes at 80°C to promote the polymerization reaction between resorcinol and formaldehyde. In the meanwhile, Si nanoparticles (<100 nm) were dispersed into DMF by ultrasonication. Then the obtained solution was added into the dispersion and underwent ultrasonic treatment. The mixture was dried and further cured in an oven at 100°C for 24 h. Finally, the polymer/Si composite was carbonized with a heating ramp of 2°C/min in flowing argon at 400°C for 3 hours and then 700°C for an additional 3 hours. For comparison, porous carbon without Si was synthesized using the same procedure described above.

The distribution of Si nanoparticles in the porous C/Si composite and the pore structure of porous C were examined by transmission electron microscopy (TEM, JEOL 2100F, Japan). Figure 3 shows the images. It can be seen that Si nanoparticles are uniformly distributed in the porous carbon matrix. Figure 3b clearly displays the porous structure of the carbon matrix in which Si particles are imbedded. The porous structure provides additional space to accommodate the huge volume change of Si nanoparticles during lithiation/delithiation reactions. The elastic carbon frame would benefit to release the strain caused by the volume change.

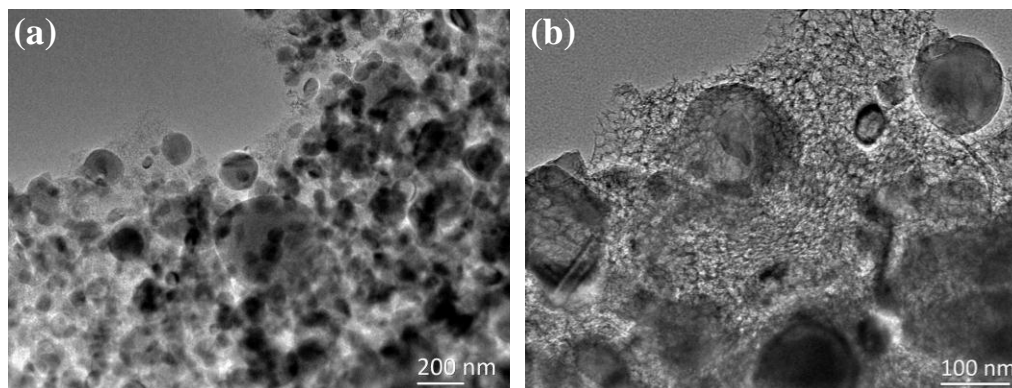


Figure 3. TEM images of porous C/Si composite.

The porous structure was further characterized by N₂ adsorption measurement. Fig. 4 depicts the adsorption isotherm. The Brunauer - Emmett - Teller (BET) specific surface area and pore volume of the porous C/Si composite are 210 m²/g and 0.29 cm³/g, respectively. The pore size distribution was analyzed by the Barrett - Joyner - Halenda (BJH) method. The results show that the average pore size is 9.8 nm, which is in accordance with those RF porous carbons. The large specific surface area and pore volume would alleviate strain and improve the electrochemical reaction kinetics.

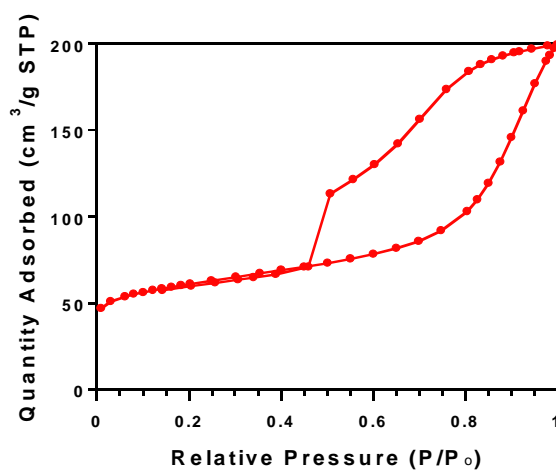


Figure 4. N₂ adsorption/desorption isotherm.

The composition of the porous C/Si composite was checked using TGA analysis in air. Figure 5 shows the thermogravimetric curve of the porous C/Si composite. One can see that no weight change is observed below 450°C. A sharp decrease occurred between

450°C and 580°C, which is due to the carbon decomposition. The slight increase in the high temperature range should result from Si oxidation. From these results, the content of Si is calculated at 76% in the composite.

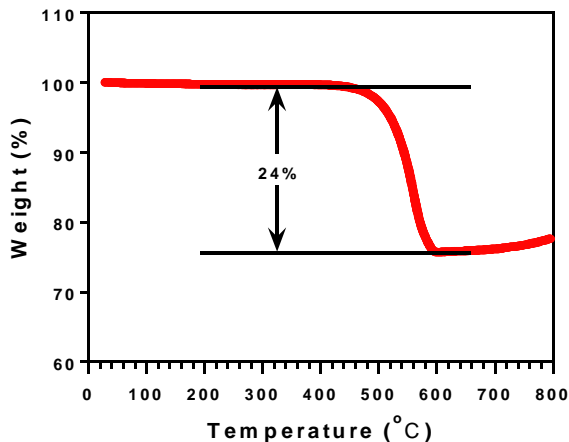


Figure 5. Thermogravimetric (TGA) curve of porous C/Sn composite in air.

Electrochemical performance characterization

Electrochemical performance of the nano-Si dispersed in porous carbon matrix electrodes was evaluated in two-electrode coin cells using lithium as the counter electrode. The porous C/Si composite was mixed with carbon black and sodium carboxymethyl cellulose (CMC) binder to form a slurry at the weight ratio of 70:15:15. The electrode was prepared by casting the slurry onto copper foil using a doctor blade and dried in a vacuum oven at 100°C overnight. Coin cells were assembled with lithium foil as the counter electrode, 1M LiPF₆ in a mixture of ethylene carbonate/diethyl carbonate (EC/DEC, 1:1 by volume) as the electrolyte, and Celgard®3501 (Celgard, LLC Corp., USA) as the separator. Cells with pure porous carbon electrodes were also fabricated using the same procedure. Electrochemical performance was tested using an Arbin battery test station (BT2000, Arbin Instruments, USA). Batteries were scanned between 0.02 – 1.5 V at a current density of 200 mA/g. Capacity was calculated on the basis of Si nanoparticle mass.

Figure 6a shows the cycling stability of the nano-Si dispersed in porous carbon electrodes. For comparison, the cycling behavior of Si nanoparticles (used in the porous C/Si composite) was also evaluated in the same conditions. The results show that the

cycling stability of porous C/Si composite is significantly improved. The porous C/Si composite delivered a reversible capacity of 1660 mAh/g in the first cycle, and retained a capacity of 707 mAh/g even after 100 charge/discharge cycles, which is still almost two times higher than graphite (theoretical capacity: 372 mAh/g). In contrast, although bare Si nanoparticles show a little higher reversible capacity of 1748 mAh/g in the first cycle, only 244 mAh/g remained after 100 cycles. No doubt the enhanced cycling stability is related to the porous structure. The large pore space can digest the volume expansion produced by the lithiation reaction. In the meanwhile, the elastic carbon matrix frame can release the strain during cycling, avoiding or reducing the pulverization of Si nanoparticles.

Figure 6b shows the charge/discharge profile of the porous C/Si composite in the 1th, 2nd, 3rd and 5th cycle. A large irreversible capacity of 1091 mAh/g was observed in the first cycle with a coulombic efficiency of 60%. This should be contributed to the irreversible reaction due to the formation of SEI film on the large electrode surface. In the consequent cycles, the coulombic efficiency is higher than 95%, indicating a good reversibility of the porous C/Si composite. These results show that incorporating nanoparticles into a porous carbon matrix is an efficient way to improve electrochemical performance for lithium ion batteries.

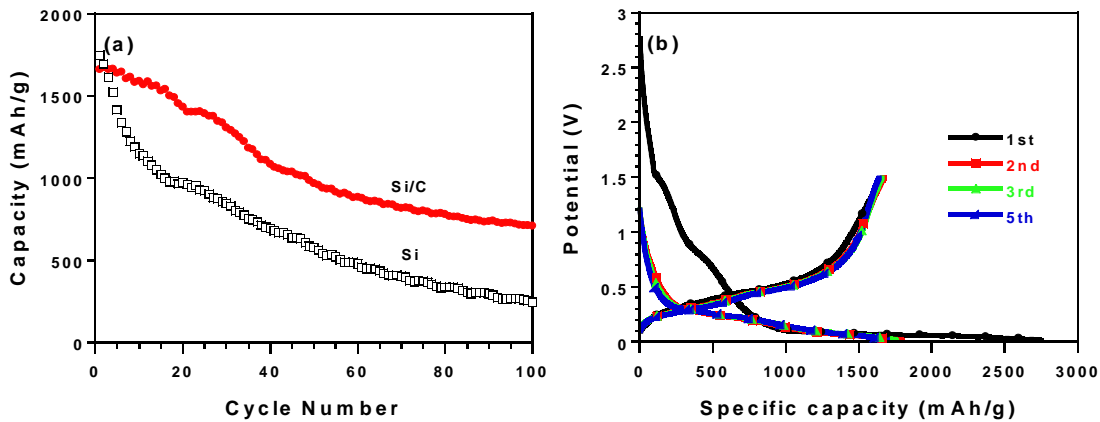


Figure 6. (a) Cycling performance of the porous C/Si composite (solid red circle) and pure Si nanoparticles (open black square). (b) Charge/discharge profiles in the 1st, 2nd, 3rd and 5th cycles.

4.3. Nano-Sn dispersed in porous carbon matrix

Two methods have been used to synthesize the C/Sn nanoporous anodes. The first method is carbonization of SnO/co-polymer, and the second method is spray pyrolysis.

Synthesis of C/Sn composites using carbonization of SnO/copolymer

The porous C/Sn composite materials is synthesized using the same procedure to prepare the porous C/Si composite, except that Si nanoparticles were replaced with SnO₂ nanoparticles (<100 nm, Sigma-Aldrich). SnO₂ nanoparticles were reduced to Sn nanoparticles during carbonization.

Fig. 7a shows the SEM image of the porous C/Sn composite. It is clearly seen that tin nanoparticles with a particle size of around 100 nm are uniformly embedded in a sponge-like porous carbon matrix. Pores with diameters of around 10 nm are separated by very thin carbon walls. The unique sponge-like carbon matrix will provide large void space and mechanical support to release strain induced by the alloying/dealloying of tin, thus preventing pulverization of tin particles.

Sn particle size and distribution in the carbon sponge was also examined using TEM, shown in Fig. 7b and 7c. Sn nanoparticles with an average particle diameter of about 100 nm were uniformly dispersed in a porous carbon matrix, which is consistent with SEM results. The particle size is similar to that of SnO₂ nanoparticles which were used as the tin source, demonstrating that the Sn nanoparticles were well dispersed and confined in the carbon matrix, and no aggregation occurred even when Sn became liquid during carbonization at a temperature higher than the melting point of tin metal. These results suggested that the sponge-like carbon matrix may prevent the aggregation of tin particles during prolonged cycling, improving cycling stability. High-resolution transmission electron microscopy (HRTEM) and selected area electron diffraction (SAED) images (Fig. 7c and insert) revealed that Sn nanoparticle is in a crystalline structure, which was also confirmed by the X-ray diffraction (XRD) pattern (Fig. 8). All the peaks in Fig. 8 could be indexed to crystal tin (JPCDS card No. 86-2264). No peaks attributed to SnO₂ were detected, indicating that the SnO₂ particles were completely converted to crystal tin.

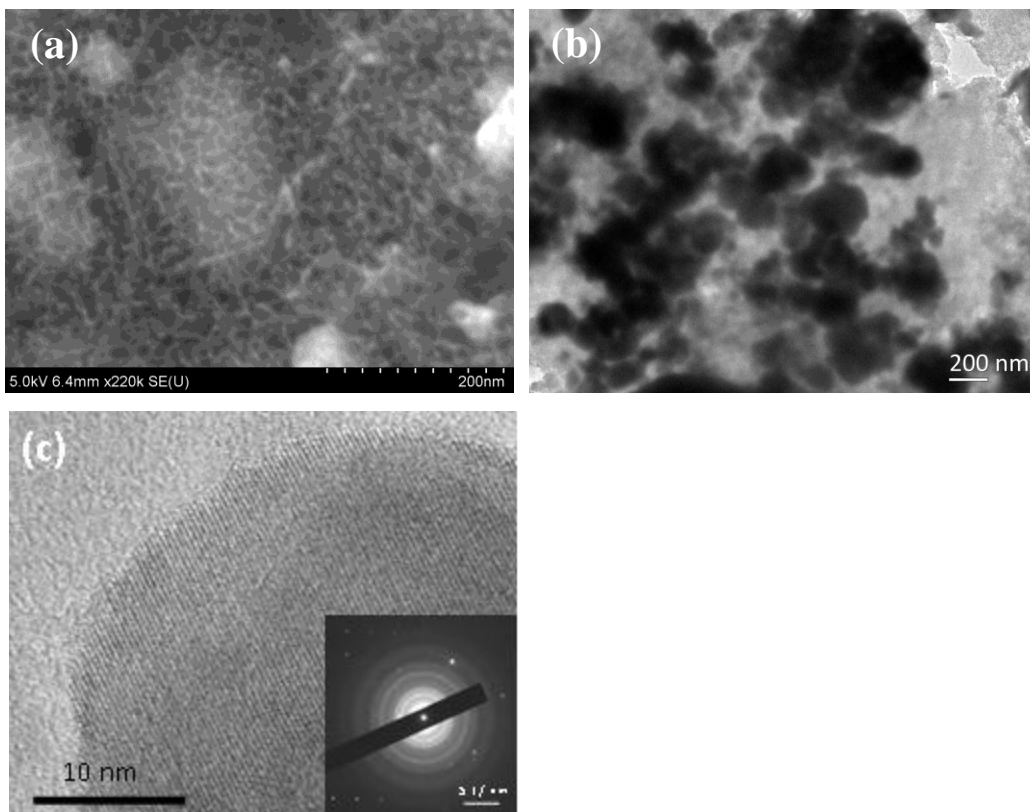


Figure 7. (a) SEM, (b) TEM, and (c) HRTEM images of the porous C/Sn composite. Insert: SAED pattern of tin nanoparticles.

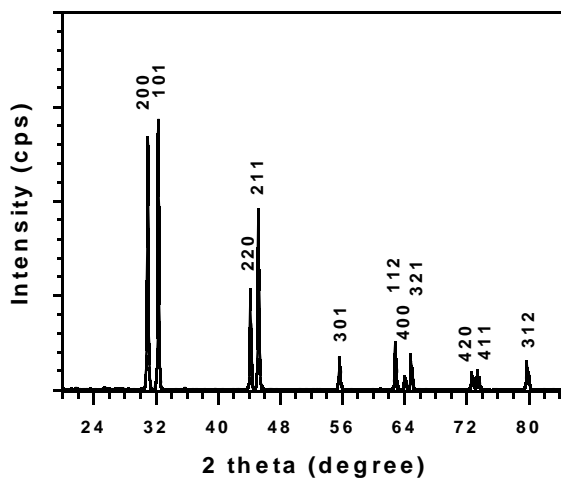


Figure 8. XRD pattern of the porous C/Sn composite. The diffraction peaks for tin (card number) was indexed in XRD pattern.

The porous structure of the C/Sn composite was characterized by N₂ adsorption measurement. Fig. 9 depicts the adsorption isotherm and the pore size distribution

analyzed by the Barrett - Joyner - Halenda (BJH) method. The Brunauer - Emmett - Teller (BET) specific surface area of the porous C/Sn composite is 180 m²/g and the pore volume is 0.16 cm³/g. BJH average pore diameter is 7 nm (Fig. 9b), which is similar to the porous C/Si composite. The large specific surface area and pore volume would be beneficial to alleviate strain, accommodate volume changes, and improve the kinetics.

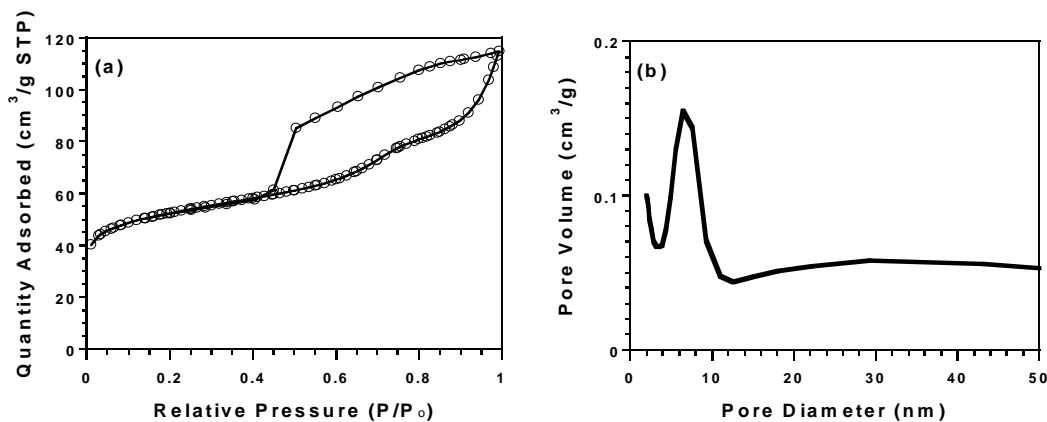


Figure 9. (a) N₂ adsorption/desorption isotherm and (b) pore-size distribution curve of the porous C/Sn composite.

Thermogravimetric analysis (TGA) was carried out using a thermogravimetric analyzer (TA Instruments, USA) with a heating rate of 10°C/min in air. Composition and thermal/chemical stability of the porous C/Sn composite was analyzed (shown in Fig. 10). The small weight loss below 100°C in Fig. 10 was attributed to water evaporation. Almost no weight loss between 100°C to 220°C can be observed, demonstrating that both carbon and Sn in porous C/Sn composite are thermally and chemically stable in air up to 220°C, i.e. no Sn oxidation reaction and carbon decomposition occurred in air at 220°C. Therefore, the sponge-like mesoporous carbon/Sn composite prepared using the soft-template method can be stored for a long-time without performance decline. The weight gain from 220°C to 300°C is attributed to the oxidation of metallic tin ($Sn + O_2 \rightarrow SnO_2$), while the weight loss from 300°C to 480°C is mainly due to carbon decomposition ($C + O_2 \rightarrow CO_2$ (gas)). The content of metallic tin in the composite was determined to be 66% using the following Equation 1:

$$Sn \text{ (wt\%)} = 100 \times \frac{\text{molecular weight of Sn}}{\text{molecular weight of SnO}_2} \times \frac{\text{final weight of SnO}_2}{\text{initial weight of C/Sn composite}} \quad (1)$$

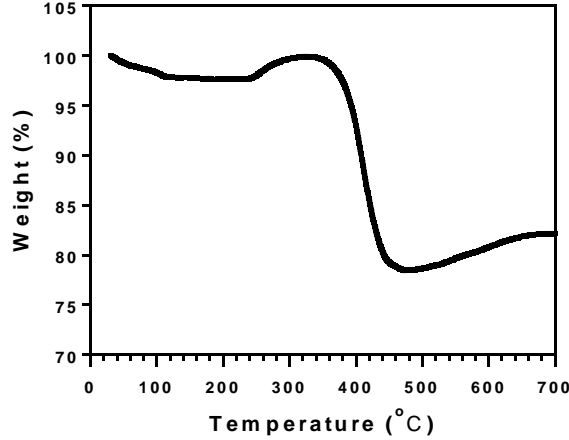


Figure 10. Thermogravimetric (TGA) curve of porous C/Sn composite in air.

Electrochemical performance of Sn/C prepared using carbonization of SnO/copolymer

Electrochemical behavior of the porous C/Sn composite electrodes were investigated in coin-style half cells using lithium as the counter electrode. The porous C/Sn composite was mixed with carbon black and sodium carboxymethyl cellulose (CMC) binder to form a slurry at the weight ratio of 70:15:15. The electrode was prepared by casting the slurry onto copper foil using a doctor blade and dried in a vacuum oven at 100°C overnight. Coin cells were assembled with lithium foil as the counter electrode, 1M LiPF₆ in a mixture of ethylene carbonate/diethyl carbonate (EC/DEC, 1:1 by volume) as the electrolyte, and Celgard@3501 (Celgard, LLC Corp., USA) as the separator. Cells with pure porous carbon electrodes were also fabricated using the same procedure. Electrochemical performance was tested using an Arbin battery test station (BT2000, Arbin Instruments, USA). Capacity was calculated on the basis of the total mass of the porous C/Sn composite. Cyclic voltammogram scanned at 0.2 mV/s between 0 – 3 V was recorded using a Solatron 1260/1287 Electrochemical Interface (Solartron Metrology, UK).

Fig. 11a shows the cyclic voltammograms in the first five cycles. Two reduction peaks at 0.33 V and 0.6 V, are assigned to the lithiation reaction between tin and lithium

to form Li_xSn alloy. The corresponding oxidation peaks between 0.4 V and 0.8 V were assigned to the delithiation reaction of Li_xSn alloy. The peak currents due to lithiation/delithiation of Sn were stabilized after an initial small decline in the first three charge/discharge cycles. Two irreversible peaks at 1.05 V and 1.55 V, responsible for the catalytic decomposition of the electrolyte on tin, were not observed during the first lithiation. Therefore, it indicated that tin nano-particles were completely encapsulated in the carbon matrix. The reason for the abnormal peak near 3 V, which occurred only in the first oxidation scan and also reported on the C/Sn composite by other researchers, is still not fully understood.

Fig. 11b illustrated the cycling stability of the porous C/Sn composite at the current density of 200 mA/g between 0.02 – 3 V. For comparison, the cycling behavior of porous carbon without tin nanoparticles was also evaluated at the same conditions. Theoretical capacity of the porous C/Sn composite (Sn:C=66:34), based on the theoretical capacity of metallic tin (992 mAh/g) and the actual capacity of pure porous carbon (335 mAh/g) in the first-cycle, was also shown in Fig. 11b. The capacity of porous C/Sn composite in the first delithiation was 769 mAh/g, which was close to the theoretical capacity of the Sn and carbon composite (770 mAh/g). The specific capacity of the C/Sn composite gradually decreased to 620 mAh/g during the initial 30 charge/discharge cycles, and then began to increase before stabilizing at 1300 mAh/g after 300 cycles. Since the capacity of pure porous carbon continuously increased with charge/discharge cycles, the initial capacity decline of porous C/Sn anodes should be attributed to slight degeneration of nano-Sn particles. The stabilized capacity of 1300 mAh/g after 300 cycles is much higher than that of current commercially used graphite and even higher than the theoretical capacity of the composite 770 mAh/g). The similar capacity increasing behavior during charge/discharge cycles has also been reported on porous carbon, SnO_2 /graphene nanocomposite, and Si/C nanocomposite anode materials in lithium ion batteries. The mechanism behind this is still not clear. Extra capacity over the theoretical capacity was also found in metal oxide anodes, where the extra capacity was attributed to reversible formation of polymeric species at 0.8 V and dissolution above 2.1 V in alkyl carbonate solution due to the high catalytic activity of metal oxides nanoparticles. The coulombic efficiency of porous C/Sn anodes increased quickly from

75% to almost 100% after 8 cycles. The porous C/Sn synthesized using simple carbonization technology showed higher capacity and longer cycle life than those C/Sn anodes reported in the open literature.

To investigate the mechanism of the extra capacity in the porous C/Sn anode, the charge/discharge behaviors at different cycles were examined. Fig. 11c shows the charge/discharge behavior of the mesoporous Sn/Carbon composite anodes in the 1st, 30th, 60th, 100th, and 150th cycles. Since the lithiation curves of the mesoporous C/Sn was interfered by SEI formation during the initial few cycles, delithiation curves were examined for mechanism of the extra capacity. The first delithiation curve consists of three small plateaus at potential around 0.6-0.8V due to the formation of Li_xSn alloys, followed by a sloped line due to lithiation of porous carbon. The decrease in delithiation capacity in the initial 30 cycles is mainly attributed to the reduced capacity of Li_xSn at a plateau potential of 0.8 V, as evidenced by the parallel delithiation curves of the first and the 30th cycles above 0.8 V. During further cycles, the capacity of Li_xSn alloy was stable. However, the capacity above 1.2 V gradually increased. Here we attributed the increased capacity above 1.2 V to reversible decomposition of gel-like polymer. The morphology of gel-like polymer on porous C/Sn anodes before decomposition was investigated using TEM after charging the electrode to 1V (Fig. 11d). A thick layer of gel-like polymer was clearly observed on the surface of the composite anode. The extra capacity over the theoretical capacity due to reversible formation of polymeric species at 0.8 V and dissolution above 2.1 V in alkyl carbonate solution was also found in metal oxide anodes. The decomposition potential (1.2 V) of the gel-like polymer on the porous C/Sn anode is much lower than those reported on CoO anodes (1.8 V). This suggests that Sn has higher catalytic activity for the reversible formation/decomposition of gel-like polymer than the transition metals. The high catalytic role of Sn was also evidenced by the faster capacity increase in the mesoporous C/Sn than in the pure porous C anodes (Fig. 11b). It should be pointed out that the capacity delivered by the gel-like polymer on transition metal oxide anodes suffered a fast capacity fading after 100 cycles, while the cycling stability of the mesoporous C/Sn composite was significantly improved, which was stabilized at 1300 mAh/g after 300 cycles.

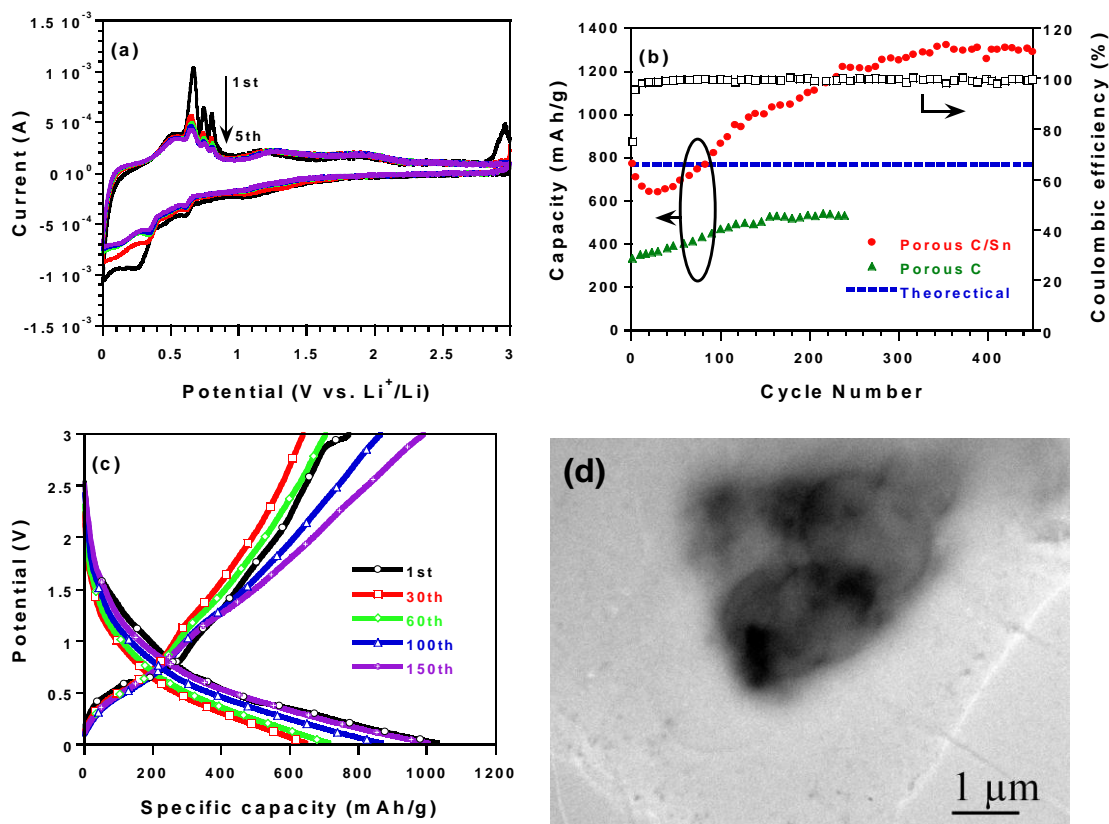


Figure 11. (a) Cyclic voltammograms of initial 5 cycles of the porous C/Sn. (b) Cycling performance of the porous C/Sn composite (red circle), porous carbon without tin nanoparticles (green triangle) and the theoretical capacity of the porous C/Sn composite based on the capacity of pure porous carbon and the theoretical capacity of metallic tin (blue dashed line). (c) Charge/Discharge profiles at the 1st, 30th, and 100th, and 150th cycle. (d) TEM image of porous C/Sn anode charged to 1 V.

After the mesoporous Sn/carbon anodes were stabilized by charging/discharging for 100 cycles at 200 mA/g, the rate capability of the porous C/Sn composite was investigated at different currents. The excellent rate performance of porous C/Sn anodes was demonstrated in Fig. 12. A high capacity of 360 mAh/g was retained at the current density of 2000 mA/g, which is much higher than reported rate performance of C/Sn composite anodes using an electrostatic spray deposition (ESD) technique. Even at a higher current of 4000 mA/g, the capacity retention is still as high as 180 mAh/g. The enhanced rate capability is believed to be associated with the unique porous structure. The thin resilient carbon walls provide a mechanical support to enable good electric contact between tin particles and carbon matrix. In addition, the large specific surface

area ensures a high electrode-electrolyte contact area, which could significantly improve the transport for electrons and lithium ions.

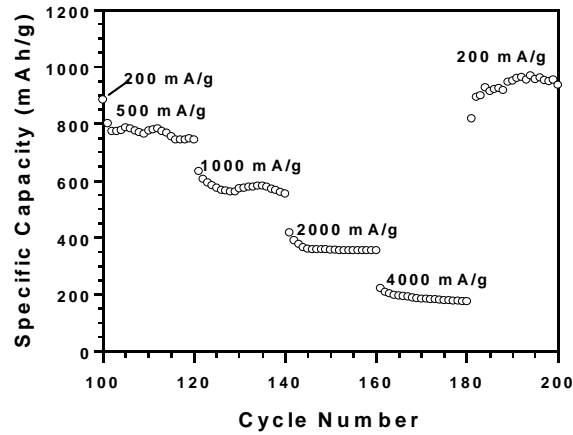


Figure 12. Rate capability of the porous C/Sn composite at different current densities and 0.02 – 3 V after 100 cycles at 200 mA/g.

C/Sn composites synthesized using a spray pyrolysis method

Sn/C composite spheres were also synthesized using a spray pyrolysis method as illustrated in Figure 13. The solution containing carbon and tin sources was atomized with argon/5% hydrogen in a collision-type nebulizer, and subsequently dried with a silica gel diffusion dryer, before entering two tubular furnaces both at 900 ° C. The nominal residence time in the heated region is ~1 s for each furnace. Thermal decomposition of tin source and carbonization of carbon source polymer yield Sn/C composite spheres. The final product, Sn/C composite spheres, was collected on a 0.4 μm (pore size) DTTP Millipore filter.

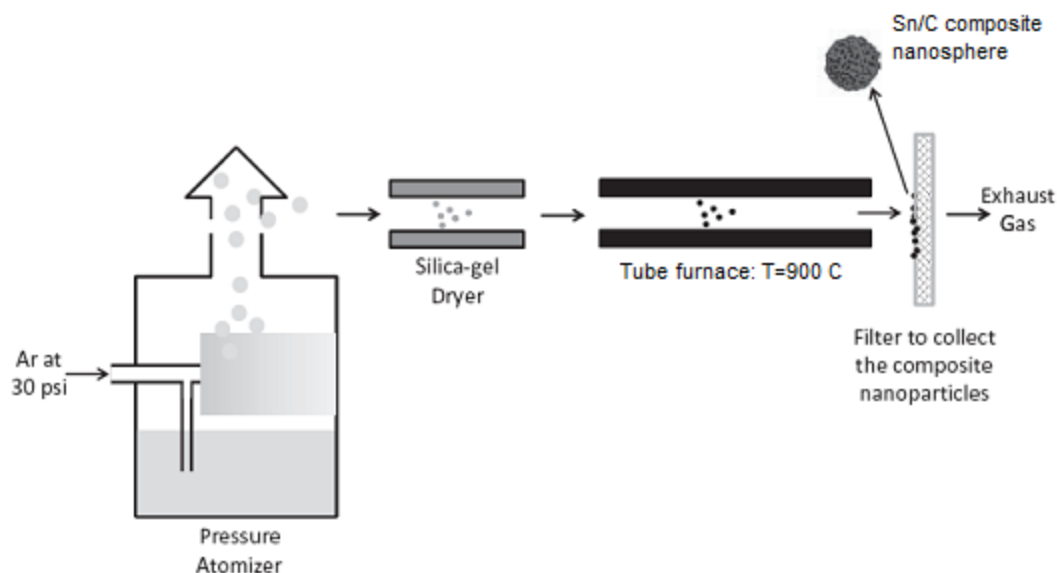


Figure 13. Diagram of the aerosol spray pyrolysis apparatus.

TEM images of the Sn/C composite nanospheres were shown in Figure 14. One can clearly see that tin nanoparticles with diameter of around 10 nm are uniformly embedded in larger spheres with size of 400 nm. Figure 14b shows a thin carbon layer of 10 nm coated on the surface of the composite spheres. High-resolution transmission electron microscopy (HRTEM) image (Figure 14c) demonstrates a crystal structure of the tin nanoparticles, which is further confirmed by XRD analysis. The results suggests that the carbon source first decomposed to create a carbon frame, which blocked tin particle growth and confined them in the carbon frame. XRD pattern of the Sn/C composite spheres is shown in Figure 15. The peaks are indexed to a tin crystal structure (JCPDS card No.: 862265). No SnO₂ was detected in the Sn/C composite spheres.

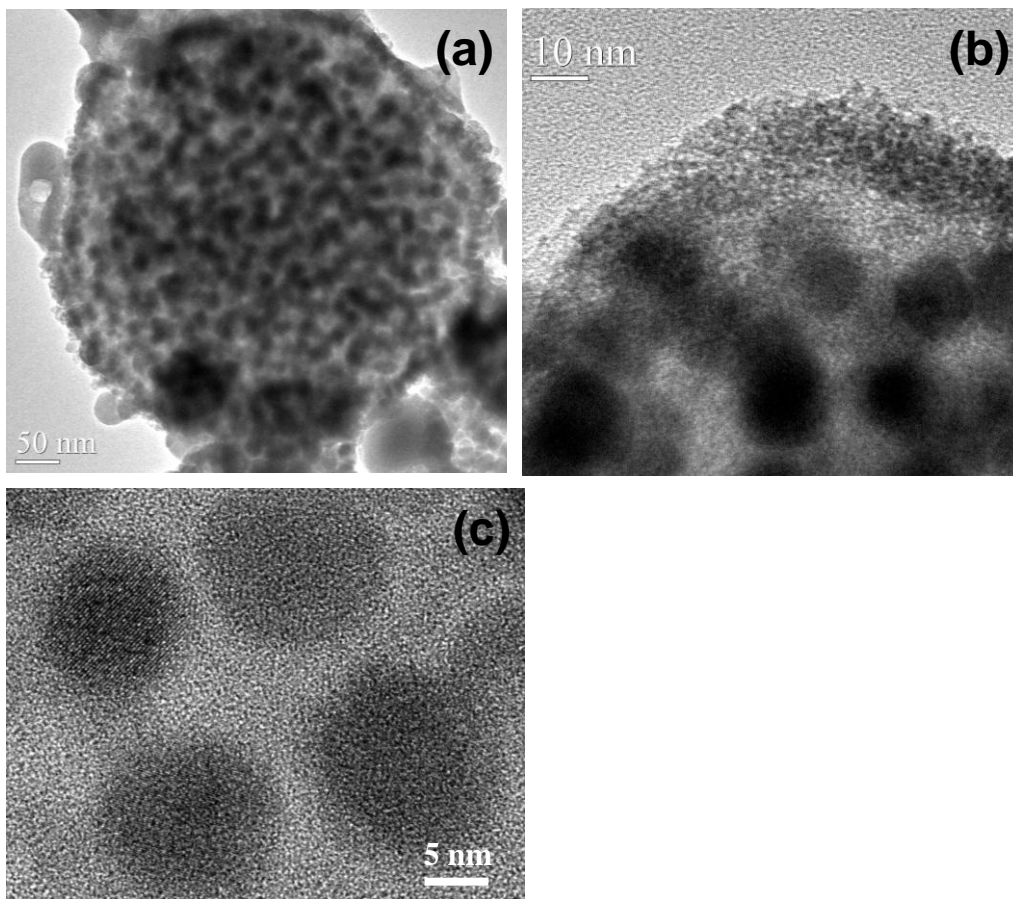


Figure 14. TEM images of Sn/C composite.

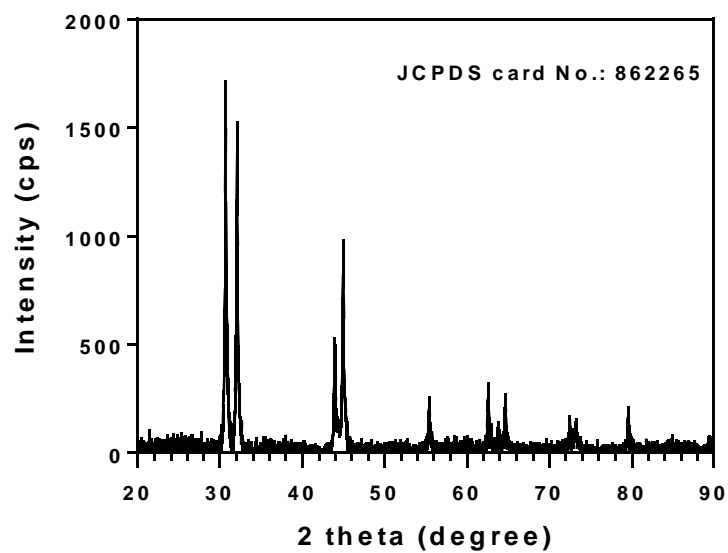


Figure 15. XRD pattern of the Sn/C composite spheres. The diffraction peaks for tin was indexed to tin crystal (JCPDS card No.: 862265).

Electrochemical performance of C/Sn composites synthesized using a spray pyrolysis method

Electrochemical behavior of the Sn/C composite sphere electrodes were investigated using the same method described above. The anode consisting of 70% Sn/C composite spheres, 15% conductive agent (carbon black) and 15% binder (sodium carboxymethyl cellulose, CMC) was cast onto copper foil and dried in a vacuum oven at 100°C overnight. Coin cells were assembled with lithium foil as the counter electrode, 1M LiPF₆ in a mixture of ethylene carbonate/diethyl carbonate (EC/DEC, 1:1 by volume) as the electrolyte, and Celgard®3501 (Celgard, LLC Corp., USA) as the separator. Cells were cycled between 0.02 – 3 V at a current density of 230 mA/g using an Arbin battery test station (BT2000, Arbin Instruments, USA).

Figure 16a illustrates the cycling stability of the porous Sn/C composite spheres. The initial reversible capacity is 710 mAh/g. It decreases to 640 mAh/g in the first 10 cycles, and then stabilizes until 60 cycles. The charge/discharge curves in the initial 3 cycles are shown in Figure 16b, demonstrating a typical tin delithiation plateau. The superior cycling performance is attributed to three unique features of the Sn/C composite spheres. First is the small size of tin nanoparticles. It has been shown that reduced particle size can significantly reduce the strain and improve electrochemical properties of electrode materials. In this work, 10 nm tin particles are believed to efficiently alleviate the strain during electrochemical reactions. Second is the porous carbon frame, which benefits to release strain, to accommodate volume change, and to integrate the whole structure together. Finally, a uniform distribution of tin nanoparticles in the carbon frame is an important factor to enhance electrode performance.

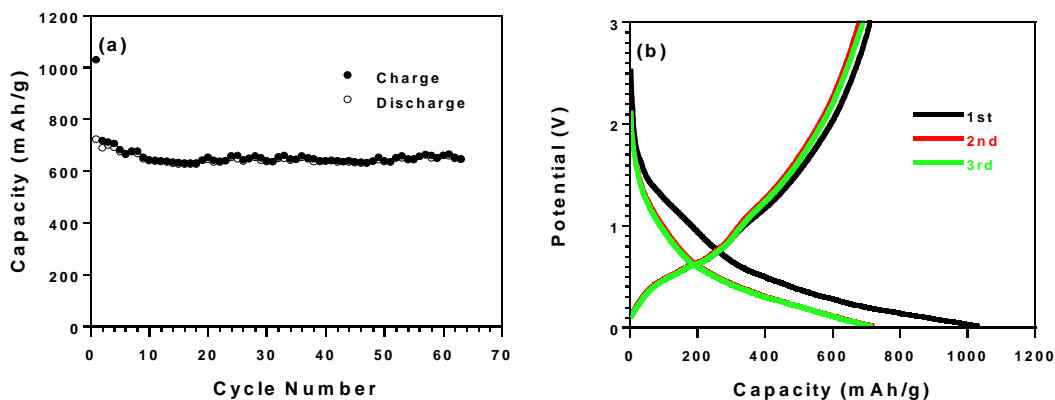


Figure 16. (a) Cycling performance of the Sn/C composite and (b) charge/discharge profiles for the initial 3 cycles.

4.4 Porous C/S composite cathode for lithium and sodium ion batteries

Synthesis and characterization of carbon/sulfur composite cathode

Sucrose was used as the carbon source and dissolved in 6 M sulfuric acid to form 5% sucrose solution, which was refluxed in a round bottom flask at 120 °C for overnight. The resulting black suspension was filtered and washed with distilled water several times. The product was dried at 100 °C in air for 24 h, and then carbonized at 1000 °C for 3 h with a heating rate of 5 °C/min under a flowing argon atmosphere. The prepared carbon spheres were mixed with sublimed sulfur (Sigma-Aldrich, USA) and sealed in glass tubes under vacuum. The tubes underwent heat treatment at 600°C for 10 h. At this temperature, sulfur is in a gas state. Sulfur was impregnated into porous carbon when cooling down. This method has been shown to be an efficient way to synthesize S/C composite electrode materials for lithium ion batteries.

Figure 17 shows the SEM images of the resulting porous carbon. It is found that porous carbon is in a sphere shape with a diameter of about 400 nm. The porous carbon sphere structure was confirmed by TEM characterization on the porous carbon/sulfur composite (Figure 18). EDS mapping images (Figure 18b and 18c) revealed that sulfur was uniformly dispersed in the porous carbon spheres. No elemental sulfur peak pattern was observed in XRD pattern. This suggests that sulfur impregnated into the porous

carbon spheres is uniformly and strongly adhered to the carbon surface in a very thin layer of coverage or in a smaller molecule than that of the regular S_8 state.

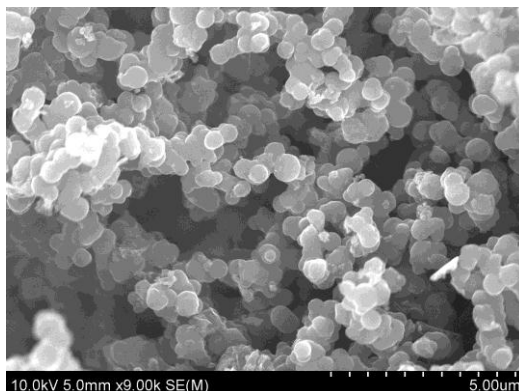


Figure 17. SEM image of porous carbon.

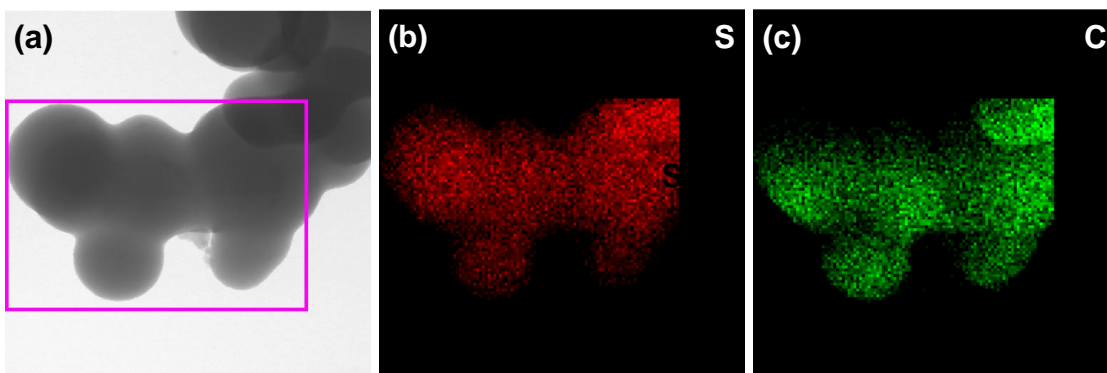


Figure 18. (a) TEM image of the porous C/S composite. (b) and (c) Elemental mapping images of S and C for the marked region in (a).

Electrochemical performance of carbon/sulfur composite cathodes for Li-ion batteries

Electrochemical behavior of the porous carbon sphere/sulfur cathodes for lithium ion batteries and sodium ion batteries were investigated. The electrode with a component of 70% C/S composite, 15% conductive agent (carbon black) and 15% binder (sodium carboxymethyl cellulose, CMC) was cast onto aluminum foil and dried in a vacuum oven at 60°C overnight. Coin cells were assembled. For lithium ion batteries, lithium and 1M $LiPF_6$ in a mixture of ethylene carbonate/diethyl carbonate (EC/DEC, 1:1 by volume) were used as the counter electrode and the electrolyte, respectively. For sodium ion batteries, sodium and 1M $NaClO_4$ in EC/DMC (1:1 by weight) were used as the counter electrode and the electrolyte, respectively. Celgard®3501 (Celgard, LLC Corp., USA)

was used as the separator. Cells were cycled between 1 – 3 V for Li ion batteries and 0.8 – 2.5 V for Na ion batteries, respectively, at a current density of 80 mA/g using an Arbin battery test station (BT2000, Arbin Instruments, USA).

Figure 19a shows the cycling performance of S-Li batteries made with porous C/S composite. The initial reversible capacity is 929 mAh/g. In the consequent cycles, the capacity stabilizes around 800 mAh/g. After 65 cycles, the capacity retention is still as high as 830 mAh/g, accounting for 89% of the initial capacity, thus showing good stability of the porous C/S composite. High coulombic efficiency approaching 100% was demonstrated except for the first cycle. The large irreversible capacity in the first cycle is generally contributed to the irreversible reaction related to the formation of SEI film.

Figure 19b depicts charge/discharge curves of the porous C/S composite in the first three cycles. Typically, lithiation of S₈ sulfur should have two discharge potential plateaus, one is at 2.4 V and the other at 2.05 V, corresponding to 1.5 and 2 lithium atom reaction steps, respectively. In Figure 19b, only one potential slope in both charge and discharge was observed in the porous C/S cathode. The first discharge slope centers at 1.62 V, and then shifts to 1.65 V in the following lithiation/delithiation cycles. The charge slopes are centered at 1.95 V. The slope potential plateau at a low reaction potential was ascribed to the low-molecular elemental sulfur and lithium polysulfides in the narrow micropores of carbon spheres in organic electrolyte. In this case, the much lower slope potential suggests that sulfur exists in a smaller-molecular state and a strong interaction between porous carbon, which could change the binding energy and thus the reaction potential. The strong binding between sulfur and carbon decrease the “polysulfide shuttle reaction,” enhancing the good reversibility. The results also revealed that the preparation method of C/S composite under vacuum at high temperature is an efficient way to produce stable C/S composite cathode materials.

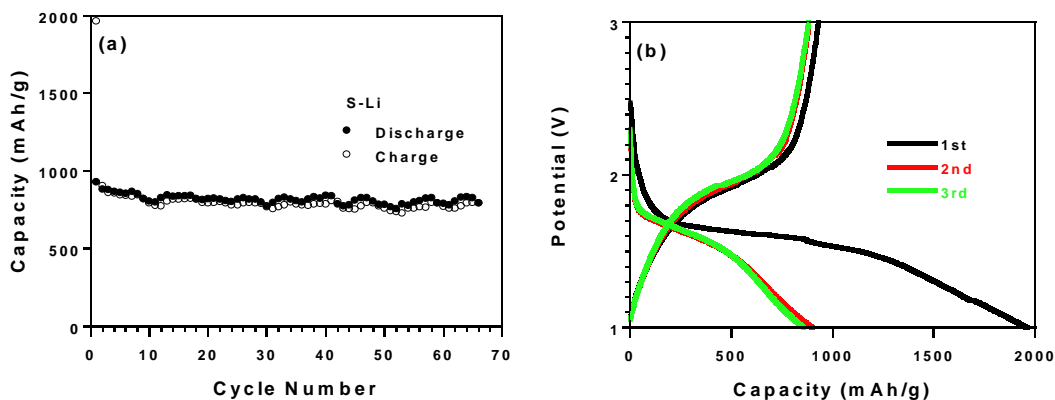


Figure 19. (a) Cycling performance of the porous C/S composite and (b) charge/discharge profiles in the initial 3 cycles for lithium ion batteries.

Electrochemical performance of carbon/sulfur composite cathode for Na-ion batteries

In addition to Li-S batteries, the electrochemical performance of C/Sn for Na-ion batteries was also investigated. Similar to Li-S batteries, excellent stability was also demonstrated for Na-S batteries (Figure 20). The first reversible capacity is 977 mAh/g, a little higher than Li-S batteries. After the first cycle, the capacity slowly decreases to a stable level of 800 mAh/g. It should be mentioned that Na ion batteries normally show worse electrochemical behaviors compared with Li ion batteries made from the same electrode materials. The size of Na atom is larger than that of Li, resulting in lower electrochemical reactivity and slower kinetics for Na-ion batteries. Here, similar electrochemical performance demonstrated that the porous C/S composite prepared using the vacuum heat treatment method can be used as cathode for both Li-ion and Na-ion batteries. Figure 20b shows the charge/discharge profiles for the initial three cycles. As Li ion batteries, only one slope potential plateau was observed in Na-ion cell, implying a similar reaction mechanism between Na-S and Li-S. It is noted that the potential for Na is 0.3 V lower than Li. The same results have been reported for Sn anodes through theoretical study, where reaction potential is 0.4 V lower for Na than Li.

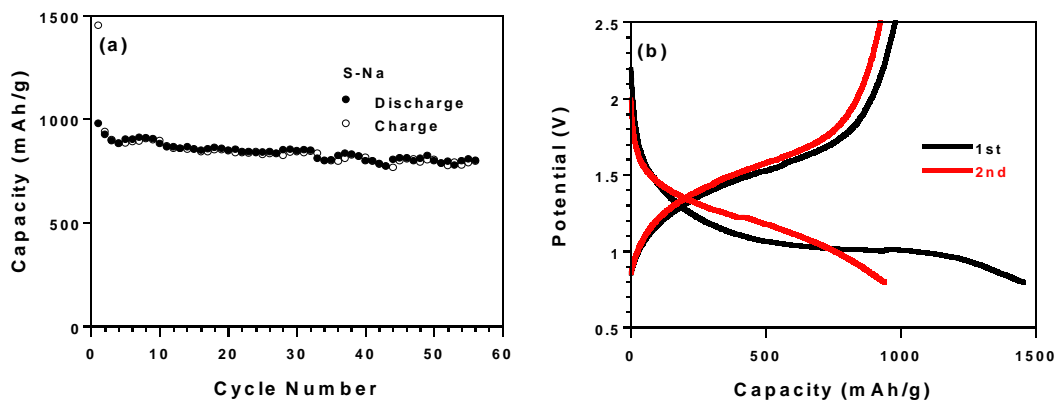


Figure 20. (a) Cycling performance of the porous C/S composite and (b) charge/discharge profiles in the initial 3 cycles for sodium ion batteries.

Summary and future plan

A series of composite electrode materials have been synthesized and characterized for lithium ion and sodium ion batteries. First, carbon-coated one-dimensional mesoporous (porous size: 50 nm) Si films was synthesized by electrochemical etching of crystalline silicon followed by CVD carbon coating. The one-dimension pore structure and carbon coating offer additional space and electric pathway to accommodate volume change and improve rate capability. The reversible capacity of over 1500 mAh/g was measured. Second, porous carbon/Si or Sn composites were synthesized by dispersing Sn or Si nanoparticles into soft-template polymer matrix followed by carbonization. These composites show enhance electrochemical performance compared to bare Si or Sn nanoparticles because the unique porous carbon structure provides space and mechanical support to accommodate the volume expansion and release stress/strain during electrochemical lithiation/delithiation. Third, homogenous Sn/C nanocomposite spheres were also synthesized using a spray pyrolysis method. Very small Sn nanoparticles (~ 10 nm) were uniformly dispersed in carbon spheres with diameter of about 400 nm. This composite spheres displayed superior cycling performance with no capacity fading after 10 cycles due to small size and uniform distribution of tin nanoparticles in carbon frame. Forth, nano-sulfur dispersed mesoporous carbon electrode materials were synthesized by high temperature S infusing method. The electrochemical properties were evaluated for lithium ion and sodium ion batteries. It is found that the nano-sulfur dispersed mesoporous carbon electrode materials show excellent electrochemical performance

bouth for both Li ion and Na ion batteries, making is attractive cathodes for next generation of rechargeable batteries. This is the first time to investigate the electrochemical properties of sulfur cathode for both Li ion and Na ion batteries.

In Year Two, fundamental research on the porous C/Si, C/Sn, and C/S synthesized in Year One will be conducted and following science questions will be answered.

1. How do porosity and pore size of the C/Si and C/Sn composites affect the electrochemical performance?
2. How do the particle size of nanoparticle and the carbon ration in the C/Si and C/Sn composites affect the cycling stability?
3. What is the reaction mechanism of C/S cathodes in lithium ion and sodium ion batteries?